NATURAL PRODUCT COMMUNICATIONS

An International Journal for Communications and Reviews Covering all Aspects of Natural Products Research

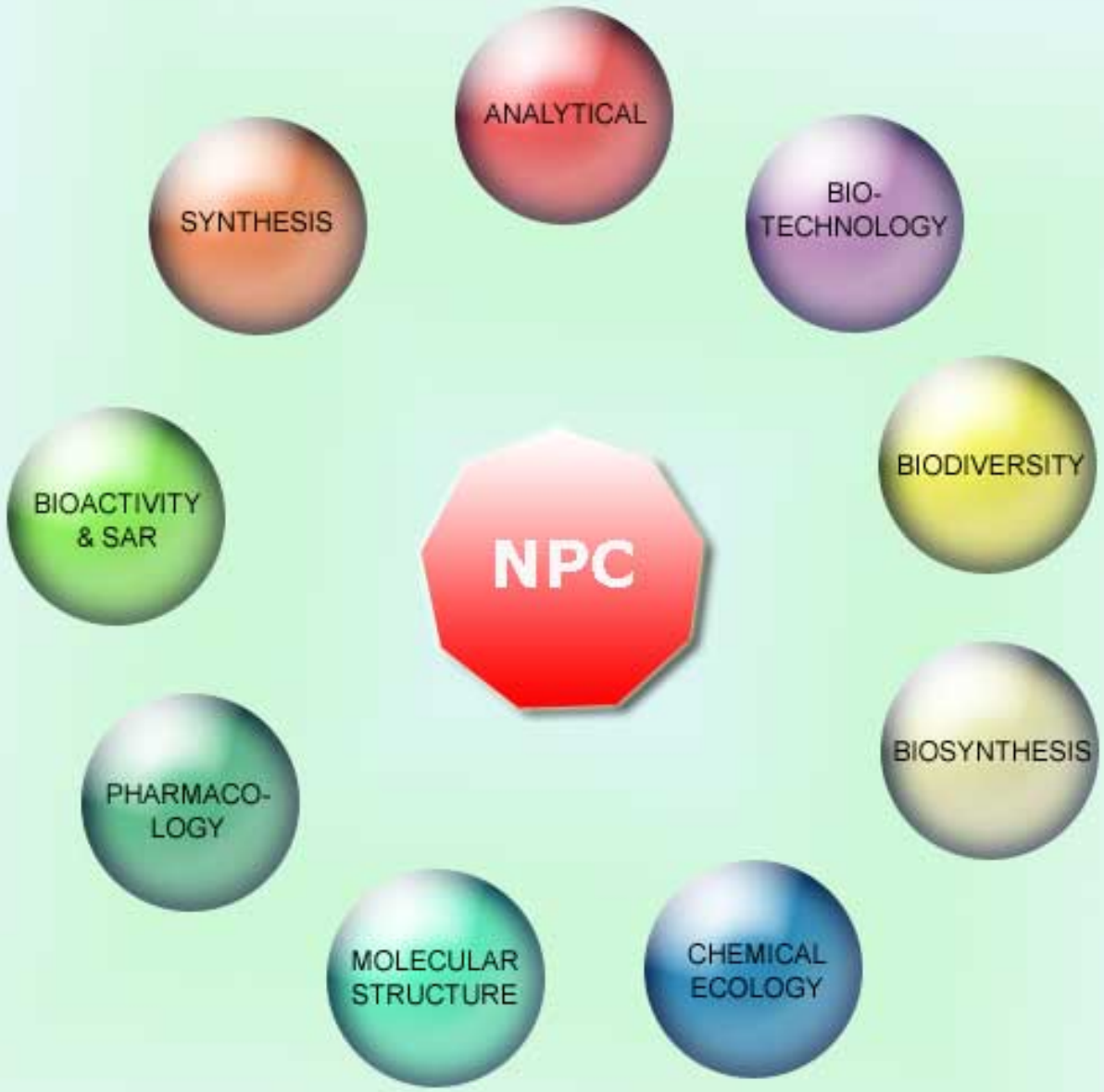

Volume 4. Issue 11. Pages 1449-1614. 2009
ISSN 1934-578X (printed); ISSN 1555-9475 (online)
www.naturalproduct.us

NPC Natural Product Communications

INFORMATION FOR AUTHORS

Full details of how to submit a manuscript for publication in Natural Product Communications are given in Information for Authors on our Web site http://www.naturalproduct.us.

To Subscribe: Natural Product Communications is a journal published monthly. 2009 subscription price: US$1,695 (Print, ISSN# 1934-578X); US$1,395 (Web edition, ISSN# 1555-9475); US$2,095 (Print + single site online). Orders should be addressed to Subscription Department, Natural Product Communications, Natural Product Inc., 7963 Anderson Park Lane, Westerville, Ohio 43081, USA. Subscriptions are renewed on an annual basis. Claims for nonreceipt of issues will be honored if made within three months of publication of the issue. All issues are dispatched by airmail throughout the world, excluding the USA and Canada.

NPC Natural Product Communications

2009
Vol. 4
No. 11
1537 - 1545

Preparation and Absolute Configuration of (1*R*,4*R*)-(+)-3-Oxo-, (1*S*,4*S*)-(-)-3-Oxo- and (1*R*,3*S*,4*R*)-(+)-3-Acetyloxy-5-oxo-1,8-cineole

María del H. Loandos,[a] Margarita B. Villecco,[a] Eleuterio Burgueño-Tapia,[b] Pedro Joseph-Nathan[c] and César A. N. Catalán[a,*]

[a]*INQUINOA-CONICET and Instituto de Química Orgánica, Facultad de Bioquímica Química y Farmacia, Universidad Nacional de Tucumán, Ayacucho 471, S. M. de Tucumán, T4000INI Argentina*

[b]*Departamento de Química Orgánica, Escuela Nacional de Ciencias Biológicas, Instituto Politécnico Nacional, Prolongación de Carpio y Plan de Ayala, Col. Santo Tomás, México, D.F., 11340 México*

[c]*Departamento de Química, Centro de Investigación y de Estudios Avanzados del Instituto Politécnico Nacional, Apartado 14-740, México, D.F., 07000 México*

ccatalan@fbqf.unt.edu.ar

Received: August 27th, 2009; Accepted: October 5th, 2009

Enantiomerically pure (1*S*,4*S*)-(-)-3-oxo-1,8-cineole (-)-**2** and (1*R*,4*R*)-(+)-3-oxo-1,8-cineole (+)-**2** were prepared for the first time and their absolute configurations assigned by vibrational circular dichroism (VCD) measurements. Thus, treatment of cineole **1** with chromyl acetate gave *rac*-**2** which after sodium borohydride reduction and acetylation provided racemic 3-*endo*-acetyloxy-1,8-cineole, *rac*-**4**. Enantioselective hydrolysis using porcine liver esterase (PLE) gave a mixture of 3-*endo*-hydroxy-1,8-cineole (-)-**3** and 3-*endo*-acetyloxy-1,8-cineole (+)-**4**. After chromatographic separation, (-)-**3** was oxidized to (+)-**2**, while (+)-**4** was hydrolysed to (+)-**3** and then oxidized to (-)-**2**. The absolute configuration of either ketone **2** was established by VCD spectroscopy in combination with density functional theory (DFT) calculations at the B3LYP/DGDZVP level of theory, from where it followed that the (+)-**2** enantiomer corresponds to (1*R*,4*R*)-1,3,3-trimethyl-5-oxo-2-oxabicyclo[2.2.2]octane and the (-)-**2** enantiomer to the (1*S*,4*S*) molecule which is also in agreement with the absolute configuration deduced by the Mosher method for the starting chiral alcohols. Some literature inconsistencies are clarified. In addition, the enantiomerically pure monoester (1*S*,3*S*,4*R*,5*R*)-(-)-3-acetyloxy-5-hydroxy-1,8-cineole **6** and the ketoester (1*R*,3*S*,4*R*)-(+)-3-acetyloxy-5-oxo-1,8-cineole **7** were prepared from *meso*-diacetate **5** by enantioselective asymmetrization also using PLE.

Keywords: (+)-3-oxo-1,8-cineole, (-)-3-oxo-1,8-cineole, (+)-3-acetyloxy-5-oxo-1,8-cineole, absolute configuration, vibrational circular dichroism, enantioselective hydrolysis, enantioselective asymmetrization, porcine liver esterase (PLE).

1,8-Cineole **1** (systematic name 1,3,3-trimethyl-2-oxabicyclo[2.2.2]octane), hereafter referred to as cineole, also known as eucalyptol or cajeputol, is a monoterpene oxide widely distributed in the plant kingdom. It is the main constituent of most *Eucalyptus* oils [1a-d] and several other essential oils [1e]. Due to its decongestant, antitussive and antibacterial properties [2a,b], the value of *Eucalyptus* oils for medicinal purposes is based largely on the cineole content [2c,d]. Cineole is chemically rather inert and consequently the literature on its chemistry is scarce and mostly related to the cleavage of the ether bridge to give *p*-menthane derivatives [3-7]. So far, we have developed the only chemical method available with good yield with direct regiospecific functionalization of **1** by oxidation with chromyl acetate [5,6] which affords racemic 3-oxocineole **2** owing to the symmetry of **1**.

In contrast, naturally occurring oxygenated derivatives have been reported sporadically, mainly as metabolites from living organisms fed on cineole containing food [8-11] such as in the urine of some mammals as brush-tail opossums, male koalas [9a-d], rabbits [9e], and humans after oral administration of medication containing **1** [12]. Microbial hydroxylation of **1** using *Bacillus cereus* [8c] and *Pseudomonas flava* [8b] yielded optically pure

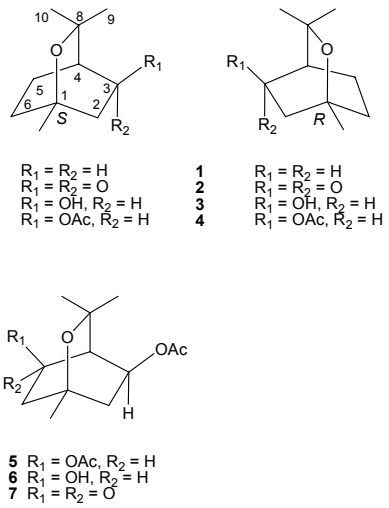

Figure 1. Chemical structures of cineole derivatives **1**-**7**.

hydroxycineole derivatives, while biotransformation of **1** by a *Rhodococcus* species, in addition to hydroxycineole derivatives, yielded optically active 2-oxocineole [13,14] of undetermined absolute configuration or enantiomeric purity. Acetyloxycineoles have been identified as the odorous components of the rhizomes of greater galangal and their enantiomeric purities determined by chiral GC [15a,b].

The racemates of *cis*- and *trans*-2- and 3-acetyloxycineoles, and the corresponding alcohols were synthesized by Kubota *et al.* [15b]. The absolute configuration of the eight possible enantiomers was determined using the (*S*)-(+)-*O*-methylmandelate esters but notably, not a single optical rotation was reported. Later, Luzzio *et al*. [16] prepared alcohol (-)-**3** by PLE-mediated hydrolysis of *rac*-**3** determining its absolute configuration as 1*R*,3*R*,4*S* by comparison of the ^{1}H and ^{13}C NMR data of the (*S*)-(+)-*O*-methylmandelate ester with those reported by Kubota [15b]. The NMR data of (*R*)-α-methoxy-α-(trifluoromethyl)-phenylacetate (MTPA) ester (Mosher esters) of both (-)-**3** and (+)-**3** were also reported [16] but remarkably, the signals are not assigned and the absolute configuration of the structures drawn for (-)-**3** and (+)-**3**, and their derivatives, are enantiomeric to that found in the literature.

The *endo-exo* nomenclature employed to name cineole derivatives seems confusing [6,9e,15c,16]. The pyrane ring of the 2-oxabicyclo[2.2.2]octane system has priority over the cyclohexane ring, and consequently the *endo-exo* descriptors must be referred to the -O-CMe$_2$- bridge. Thus, we prepared enantiomerically pure (1*S*,4*S*)-(-)-3-oxo-1,8-cineole (-)-**2** and (1*R*,4*R*)-(+)-3-oxo-1,8-cineole (+)-**2** by oxidation of the (+)-**3** and (-)-**3** alcohols, respectively, which were obtained by resolution of racemic 3-*endo*-acetyloxy-1,8-cineole *rac*-**4** with porcine liver esterase (PLE) as previously described [16,17] (Figure 1). The absolute configuration of the ketones was established from vibrational circular dichroism (VCD) measurements in comparison to density functional theory (DFT) calculations [18].

On the other hand, enantiomerically pure monoester (1*S*,3*S*,4*R*,5*R*)-(-)-3-acetyloxy-5-hydroxy-1,8-cineole **6** was prepared from *meso*-diacetate **5** by enantioselective asymmetrization also using PLE. Oxidation of **6** with pyridinium chlorochromate afforded (1*R*,3*S*,4*R*)-(+)-3-acetyloxy-5-oxo-1,8-cineole **7** (Figure 1). All these compounds are useful chiral intermediates for the preparation of other cineole derivatives as well as *p*-menthane derivatives of known absolute configuration by regioselective opening of the ether bridge [4,6]. Although ketone **2** has not yet been found in nature, it can be predicted rather confidently that it will be found as a microbial metabolite [8b,13,14].

Regioselective oxidation of **1** using chromyl acetate afforded *rac*-**2** [6] that when analyzed by chiral GC showed 49.98±0.05% of (+)-**2** (Rt 10.45 min) and 50.02±0.05% of (-)-**2** (Rt 11.53 min; see Experimental). Attempts to isolate the enantiomerically pure ketones by HPLC using a Chirex 3014 column [(S)-valine and (R)-1-(α-naphthyl)-ethylamine; Phenomenex] were unsuccessful. Then, *rac*-**4** was obtained from *rac*-**2** as described [6]. The GC trace using a chiral column (see experimental) showed 50.04±0.12% of (-)-**4** (Rt 23.4 min) and 49.97±0.12% of (+)-**4** (Rt 23.9 min) demonstrating the accuracy of the analytical methodology. Enantioselective hydrolysis using pig liver esterase (PLE) at pH 7.00 [16,17] produced a mixture of (-)-**3** along with unaffected (+)-**4** which were readily separated by column chromatography on Si gel. The progress of the enantioselective hydrolysis was monitored by GC-MS after incubation during 6, 12, 18 and 24 h showing that the reaction at 37ºC was essentially complete after 12 h. Chiral GC analysis of the unaffected acetate after 12 h showed, in three separate runs, the presence of (+)-**4** (96.0-98.5%) and (-)-**4** (1.5-4.0%). After 18 h the remaining acetate was enantiomerically pure (>98.5%) [19] while the employed chiral GC column was ineffective to resolve the enantiomers of alcohol **3**.

Table 1. NMR Data for (-)-**3** and (*R*)- and (*S*)-MTPA Esters of (-)-**3** in $CDCl_3$ (data for the MTPA moiety are not included).

	(-)-**3**		(-)-**3** (*R*)-MTPA		(-)-**3** (*S*)-MTPA		$\Delta\delta_{S-R}$ values
Position*	δ_H (*J* in Hz)	δ_C	δ_H (*J* in Hz)	δ_C	δ_H (*J* in Hz)	δ_C	
1		70.2		69.9		69.9	
2a	2.06, dd (13.6,10.3)	43.2	2.21, dd (14.3, 10.3)	40.1	2.20, dd (14.1, 10.5)	39.9	- 0.01
2b	1.69, ddd (13.6, 6.0, 3.3[┼])		1.67, m		1.81, ddd (14.1, 6.3, 3.0[┼])		+ 0.14
3	4.14 ddd (10.3, 6.0, 2.1[+])	70.9	5.23, ddd (10.3, 6.1, 2.1[+])	75.3	5.24, ddd (10.5, 6.3, 2.1[+])	75.1	
4	1.54, m	40.8	1.75, m	37.9	1.68, m	37.6	- 0.07
5a	2.03, m	21.4	2.12, m	21.2	2.12, m	21.1	
5b	1.34-1.40, m		1.54, m		1.53, m		
6a	1.58, m	30.1	1.64, m	30.0	1.65, m	29.9	
6b	1.34-1.40, m		1.45, m		1.48, m		
7	1.11, s	26.9	1.10, s	26.6	1.12, s	26.6	
8		73.4		72.9		72.8	
9	1.43, s	30.8	1.12, s	30.1	1.01, s	29.9	- 0.11
10	1.24, s	30.5	1.22, s	30.0	1.18, s	29.9	- 0.04

* a, *trans* and b, *cis* to the oxygen bridge [┼] Long-rangeW-coupled to H-6b, as evidenced by spin-spin decoupling and COSY.[+]Coupled to H-4 as evidenced by COSY.

The absolute configuration of (-)-**3** was confirmed with the aid of the Mosher methodology [20,21] and molecular modeling calculations. Compound (-)-**3** was treated with (*R*)- or (*S*)-α–methoxy-α-(trifluormethyl)phenylacetic acid to obtain its (*R*)-MTPA and (*S*)-MTPA esters, respectively. Analysis of the ^{1}H NMR data of the MTPA esters showed that $\Delta\delta H_{(S-R)}$ for H-2b and Me-9 was +0.14 and -0.11 (Table 1), respectively. This ^{1}H NMR anisotropic effects were in agreement with the minimum energy conformation of (*R*)-MTPA (**3*R***) and (*S*)-MTPA (**3*S***) esters of (1*R*,3*R*,4*S*)-**3** (Figure 2), from which can be deduced that in **3*R*** the phenyl group mainly shields H-2b, whereas, in **3*S*** the shielded group is Me-9. The minimum energy conformations were generated following a protocol which started by a Monte Carlo search at the MMFF94 [23] level. A total of 7 and 8 conformers were found for (*R*)-MTPA and (*S*)-MTPA, respectively, within a ΔE = 2 kcal/mol in the initial 10 kcal/mol range. All conformers were submitted to geometry optimization using DFT [18] calculations at the B3LYP/6-31G(d) level of theory (see Table 3) from which the **3*R*** and **3*S*** (Figure 2) were obtained as the most stable ones. The ^{1}H and ^{13}C NMR data for both Mosher esters derived from (-)-**3** are listed in Table 1.

Pyridinium chlorochromate (PCC) oxidation of (-)-**3** cleanly produced ketone (1*R*,4*R*)-(+)-**2** while the enantiomeric ketone (1*S*,4*S*)-(-)-**2** was obtained by PCC oxidation of alcohol (+)-**3** obtained after alkaline hydrolysis of acetate (+)-**4**. Chiral GC analysis showed 97.0% enantiomeric excess (ee) for (+)-**2** and 93.9% ee for (-)-**2**.

In order to gain independent evidence of the absolute stereochemistry of **2**, the theoretical VCD spectrum

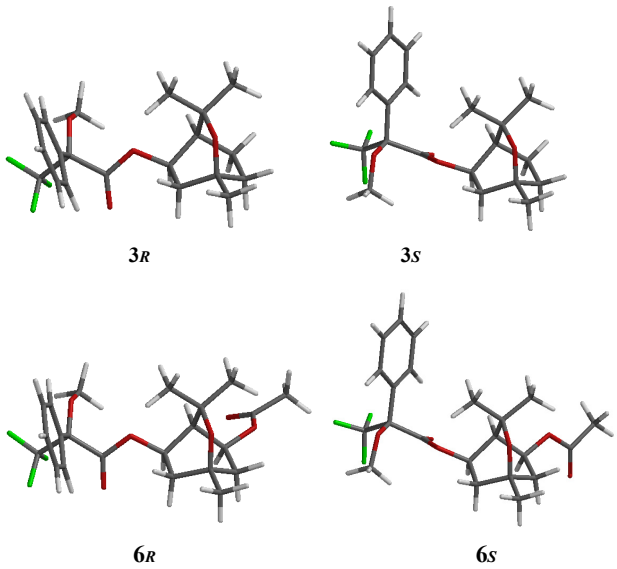

Figure 2. DFT B3LYP/6-31G(d) minimum energy conformation for (*R*)-MTPA (**3R**) and (*S*)-MTPA (**3S**) esters of (-)-**3**, and for (*R*)-MTPA (**6R**) and (*S*)-MTPA (**6S**) esters of (-)-**6**.

of (1*S*,4*S*)-**2** was obtained following a protocol which started by calculation of the global minimum energy conformation, followed by a Monte Carlo [22] search at the MMFF94 [23] level of theory. The Monte Carlo search using the global minimum as the starting point afforded a single conformer in the initial 10 kcal/mol range. This conformer was submitted to geometry optimization using DFT [18] calculations at the B3LP/6-31G(d) level of theory to obtain an accurate molecular model of (1*S*,4*S*)-**2**. After structure optimization, the IR and VCD frequencies were calculated at the B3LYP/DGDZVP level of theory, which in a basis set optimized for DFT methods [24] that has been used successfully in recent studies [25]. Detail comparison of the calculated and experimental IR frequencies provided an anharmonicity factor of 0.98. Comparison of the

Table 2. NMR Data for (-)-**6**, (*R*)- and (*S*)-MTPA Esters of (-)-**6**, and (+)-**7** in $CDCl_3$ (data for the MTPA moiety are not included)

	(-)-**6**		(-)-**6** (*R*)-MTPA		(-)-**6** (*S*)-MTPA		$\Delta\delta_{S-R}$ values		(+)-**7**	
Position*	δ_H (*J* in Hz)	δ_C	δ_H (*J* in Hz)	δ_C	δ_H (*J* in Hz)	δ_C		δ_H (*J* in Hz)	δ_C	
1			69.4		69.8		69.8			72.7
2a	2.00, dd (13.8,10.5)		41.8	2.10, dd (14.4, 10.5)	39.9	2.11, dd (14.3, 10.5)	40.0		2.34, dd (14.4,10.4)	39.7
2b	1.65-1.74, m			1.72, ddd (14.4, 5.4, 3.1†)		1.68, ddd (14.3, 5.5, 3.2)			1.92, ddd (14.4, 6.5, 3.3)	
3	4.83, ddd (10.5, 5.4, 2.2)		71.1	4.97, ddd (10.5, 5.4, 2.0)	70.9	4.96, ddd (10.5, 5.5, 2.0)	70.8		5.07, ddd (10.4, 6.5, 2.0)	66.8
4	1.94, t (2.2)		44.6	2.11, m	42.4	2.04, m	42.2	- 0.07	2.52, d (2.0)	56.8
5	4.14, ddd (10.5, 6.0, 2.2)		68.8	5.17, ddd (10.4, 5.8, 1.7)	73.4	5.17, ddd (10.5, 5.8, 1.7)	73.4			208.7
6a	1.98, dd (13.8, 10.5)		39.0	2.19, dd (14.3, 10.4)	39.8	2.19, dd (14.3, 10.5)	39.7		2.36, dd (19.0, 3.3)	48.3
6b	1.65-1.74, m			1.61, ddd (14.3, 5.8, 3.1†)		1.75, ddd (14.3, 5.8, 3.2)		+0.14	2.21, d (19.0)	
7	1.16, s		26.2	1.15, s	26.6	1.17, s	26.7		1.29, s	25.7
8			72.2		73.3		73.2			73.3
9	1.36, s		31.6	1.35, s	31.8	1.31, s	31.8	- 0.04	1.46, s	31.3
10	1.45, s		31.6	1.10, s	31.8	1.03, s	31.7	- 0.07	1.13, s	29.5
Acetyl	2.06, s		21.4	2.03, s	21.9	2.04, s	21.9		2.08, s	21.1
			170.7		170.9		179.9			169.9

* a, *trans* and b, *cis* to the oxygen bridge
† Long-range W-coupled to H-6b, as evidenced by spin-spin decoupling and COSY.

Table 3. MMFF94 and DFT B3LYP/6-31G(d) relative energy, and DFT population for the most stable conformers of MTPA ester ***3R*** and ***3S***.

3R				***3S***			
Conformer	ΔEMMFF[a]	ΔEDFT[b]	*p*DFT[c]	Conformer	ΔEMMFF[d]	ΔEDFT[e]	*p*DFT[c]
a	0.00	2.27	1.7	**a**	0.00	2.55	0.86
b	0.30	2.40	1.3	**b**	0.04	1.91	2.49
c	0.36	1.67	4.5	**c**	1.12	2.70	0.70
d	0.39	1.07	12.4	**d**	1.13	2.74	0.63
e	0.69	2.25	1.6	**e**	1.19	1.55	4.70
f	1.50	1.94	2.9	**f**	1.33	2.15	1.63
g	1.73	0.00	75.6	**g**	1.93	0.78	16.68
				h	2.07	0.00	65.70

[a]Obtained from the Monte Carlo analysis, in kcal/mol relative to ***3R*a** with *E*MMFF = 138.407 kcal/mol. [b]In kcal/mol relative to ***3R*g** with *E*DFT = -864459.605 kcal/mol. [c]DFT population in % calculated from the Boltzmann distribution equation in relation their DFT energy values. [d]Obtained from the Monte Carlo analysis in kcal/mol relative to ***3S*a** with *E*MMFF = 138.086 kcal/mol. [e]In kcal/mol relative to ***3R*g** with *E*DFT = -864460.055 kcal/mol.

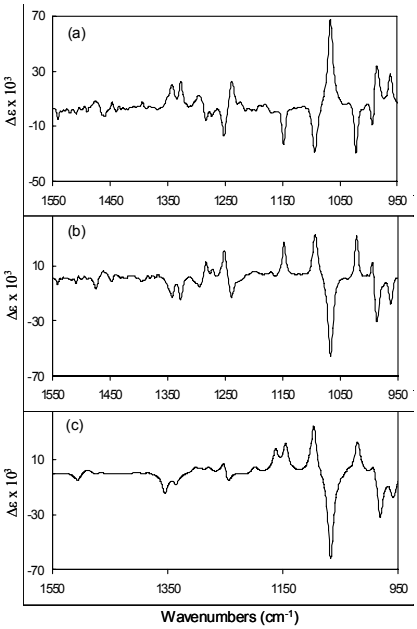

Figure 3. Comparison of observed (a) (1*R*,4*R*)-(+)-**2** and (b) (1*S*,4*S*)-(-)-**2**, and (c) calculated DFT B3LYP/DGDZVP VCD spectra of (1*S*,4*S*)-**2**.

experimental VCD spectra of (+)- and (-)-**2** with the calculated DFT B3LYP/DGDZVP VCD plot for (1*S*,4*S*)-**2** (Figure 3) directly allows to assign the 1*S*,4*S* absolute configuration to the (-)-enantiomer, in agreement with the conclusion obtained by Mosher methodology.

Symmetric 3,5-diketo-1,8-cineole and *endo-meso*-3,5-dihydroxy-1,8-cineole were prepared as described [6]. Treatment of the diol with excess acetic anhydride in pyridine afforded the corresponding *meso*-diacetate **5** which was asymmetrized using PLE to give (1*S*,3*S*,4*R*,5*R*)-(-)-3-acetyloxy-5-hydroxy-1,8-cineole **6** the absolute configuration of which was corroborated using the Mosher method [20,21] and molecular modeling. Analysis of the ^{1}H NMR data of the MTPA esters showed that $\Delta\delta H_{(S-R)}$ for H-6b and Me-10 are +0.14 and -0.07 (Table 2), respectively. The Monte Carlo protocol showed 12 conformers for (*R*)-MTPA and

Table 4. MMFF94 and DFT B3LYP/6-31G(d) relative energy, and DFT population for the most stable conformers of MTPA ester **6*R*** and **6*S***.

6*R*				**6*S***			
Conformer	Δ*E*MMFF[a]	Δ*E*DFT[b]	*p*DFT[c]	Conformer	Δ*E*MMFF[d]	Δ*E*DFT[e]	*p*DFT[c]
a	0.00	2.26	1.8	**a**	0.00	1.60	3.5
b	0.21	2.76	0.8	**b**	0.03	2.46	0.8
c	0.38	2.40	1.4	**c**	0.10	2.57	0.7
d	0.43	1.73	4.3	**d**	0.13	1.87	2.2
e	0.52	1.63	5.1	**e**	0.90	2.61	0.6
f	0.63	2.26	1.8	**f**	0.96	2.40	0.9
g	0.85	2.79	0.7	**g**	1.11	2.75	0.5
h	0.85	3.24	0.3	**h**	1.21	2.29	1.1
i	1.50	2.27	1.7	**i**	1.90	1.63	3.3
j	1.53	0.00	78.7	**j**	1.91	0.55	20.6
k	1.57	1.98	2.8	**k**	1.96	0.00	52.1
l	1.85	2.79	0.7	**l**	1.96	0.80	13.5

[a]Obtained from the Monte Carlo analysis, in kcal/mol relative to **6*R*a** with *E*MMFF = 124.305 kcal/mol. [b]In kcal/mol relative to **6*R*g** with EDFT = -1007454.64 kcal/mol. [c]DFT population in % calculated from the Boltzmann distribution equation in relation their DFT energy values. [d]Obtained from the Monte Carlo analysis in kcal/mol relative to **6*S*a** with *E*MMFF = 124.153 kcal/mol. [e]In kcal/mol relative to **3*R*k** with *E*DFT = -1007454.63 kcal/mol.

(*S*)-MTPA esters of (1*S*,3*S*,4*R*,5*R*)-**6** within the initial ΔE = 2 kcal/mol in a 10 kcal/mol range. Geometry optimization using DFT [18] calculations at the B3LYP/6-31G(d) level of theory (Table 4) conducted to the (*R*)-MTPA (**6*R***) and (*S*)-MTPA (**6*S***) conformers (Figure 2) as the most stable in agreement with observed ^{1}H NMR anisotropic effects. PCC oxidation of **6** afforded (1*R*,3*S*,4*R*)-(+)-3-acetyloxy-5-oxo-1,8-cineole **7**. The ^{1}H and ^{13}C NMR data of the latter compounds are listed in Table 2.

Experimental

General Experimental Procedures: Optical rotations were measured on a SEPA-300 HORIBA polarimeter. NMR measurements were recorded on a Bruker 300 AVANCE spectrometer at 300 (^{1}H) and 75 (^{13}C) MHz in $CDCl_3$ solutions containing TMS as internal standard. Melting points were determined on an Ernst Leitz 350 microscope. Porcine liver esterase (PLE), (*R*)- and (*S*)-α-methoxy-α-trifluormethylphenylacetic acid were purchased from Sigma-Aldrich. Merck silica gel (230-400 mesh, ASTM) was used for column chromatography (CC). Analytical TLC were performed on precoated Merk silica gel $60F_{254}$ plates. The aroma characteristics of each enantiomer were evaluated by smelling the pure compound.

Chiral GC-FID analysis: They were carried out using a Hewlett Packard 5890 Series II gas chromatograph equipped with a flame ionization detector (FID) and a chiral capillary column Cyclosil-B (30 m x 0.25 mm i.d. x 0.25 μm film thickness) (J&W Scientific). Injector and detector temperature were maintained at 250°C and 270°C, respectively. Injection size 0.5 μL, split mode, nitrogen was used as carrier gas at a flow rate of 1.00 mL min^{-1}. The oven was programmed as follows: (a) for acetates (+)-**4** and (-)-**4**: 110°C to 135ºC at 0.5ºC min^{-1}; Rt (+)-**4**: 23.89 min; Rt (-)-**4**: 23.36 min; (b) for ketones (+)-**2** and (-)-**2**, and 3-acetyloxy-5-hydroxy-1,8-cineole **6**: 125ºC (20 min), 125 → 220ºC (10ºC min^{-1}), 220ºC (10 min); Rt (+)-**2**: 10.45 min; Rt (-)-**2**: 11.53 min; Rt (+)-**6**: 33.63 min; Rt (-)-**6**: 33.80 min; (c) for (+)-3-acetyloxy-5-oxo-1,8-cineole **7**: 125 → 220ºC (2 ºC min^{-1}), 220ºC (5 min); Rt (+)-**7**: 17.94 min. Percentages (FID) were obtained from electronic integration measurements using an HP 3395 integrator.

GC-MS analysis: Mass spectra were recorded on a 5973 Hewlett Packard selective mass detector coupled to a Hewlett Packard 6890 GC using HP-5MS (5% phenylmethylsiloxane) capillary column (30 m x 0.25 mm i.d.; 0.25 μm film thickness). The injector, GC-MS interphase, ion source and selective mass detector temperatures were maintained at 250°C, 275°C, 280°C and 150°C, respectively; ionization energy, 70 eV; injection size: 1.0 μL (split mode). Helium was used as carrier gas at a flow rate of 1.0 mL min^{-1}. The oven was programmed as follows: 60°C (2 min), 60 →120ºC (1.5°C min^{-1}), 120°C (1 min), 120 → 200ºC (8ºC min^{-1}), and then held at 200°C for 5 min.

Preparation of Mosher esters: A solution of alcohol (42 μmol) in CH_2Cl_2 (2 mL) was treated with a

solution of dicyclohexylcarbodiimide (78 mg, 378 μmol), 4-(dimethylamino)pyridine (11.6 mg, 95 μmol) and either (*R*)- or (*S*)-α-methoxy-α-(trifluormethyl)phenylacetic acid (38.8 mg, 166 μmol) in CH_2Cl_2 (2 mL) at room temperature for 24 h. The reaction mixture was worked up as described for deodarols [26]. In each case, the Mosher ester was purified by flash column chromatography on silica gel using hexane-EtOAc mixtures as eluent.

General procedure for the PLE-catalyzed resolutions: The enzymatic reaction was carried out using a slightly modified known procedure [17] with a porcine liver esterase (PLE) (EC 3.1.1.1; Sigma Lot 123K7033) suspension (2,500-2,600 units) in buffer phosphate solution (pH 7.00, 15 ml), which was added to the substrate (4.70 mmol) in a single portion and then incubated at 37ºC with magnetic stirring Aliquots (0.5 mL) were taken at 6, 12, 18 and 24 h. Each sample was salted out followed by addition of ethyl acetate (1 mL), and the suspension was vigorously stirred. After centrifugal separation, the organic layer was dried over anhydrous Na_2SO_4, filtered, the solvent was removed under reduced pressure and the residue was monitored by TLC and GC-MS. After incubation for 12 h, GC-MS analysis showed 45.8% of (1*R*,3*R*,4*S*)-(-)-**3** and 54.2% of (1*S*,3*S*,4*R*)-(+)-**4** since acetate **4** is more efficiently extracted from the aqueous phase than alcohol **3**; percentages were taken directly from the area % report of the total ion chromatogram and are not corrected by detector factor response.

(1*R*,3*R*,4*S*)-(-)-3-Hydroxy-1,8-cineole (-)-**3** and **(1*S*,3*S*,4*R*)-(+)-3-acetyloxy-1,8-cineole** (+)-**4:** The general procedure was followed using 431 mg (2.03 mmol) of (±)-3-*endo*-acetyloxy-1,8-cineole **4**. After incubation for 12 h the mixture was salted out, extracted with ethyl acetate (3 x 20 mL), the organic extract was dried over anhydrous Na_2SO_4, filtered, the solvent was removed under reduced pressure and the residue containing the ester/alcohol mixture was chromatographed on Si gel with hexane-EtOAc mixtures as eluent to yield (1*S*,3*S*,4*R*)-(+)-3-acetyloxy-1,8-cineole (+)-**4** (185 mg, 43%) and (1*R*,3*R*,4*S*)-(-)-3-hydroxy-1,8-cineole (-)-**3** (142 mg, 41%), as crystalline solids (amounts and percentages are the average of three runs). Chiral GC analysis of the isolated ester showed the following composition (three separate runs): (+)-**4**, 98.5%, 98.2% and 96.0%; (-)-**4**, 1.5%, 1.8% and 4.0% respectively. After incubation for 18 h the remaining acetate was almost enantiomerically pure (>98.5%).

(1*S*,3*S*,4*R*)-(+)-3-Acetyloxy-1,8-cineole, (+)-**4**

MP: 39-40ºC (from pentane).

$[\alpha]_D$: +52.0 (*c* 1.00, $CHCl_3$), 94% ee (reported [16]: MP 41-43ºC; $[\alpha]_D$: +55.8).

(1*R*,3*R*,4*S*)-(-)-3-Hydroxy-1,8-cineole, (-)-**3**

MP: 93.5-94ºC (from pentane).

$[\alpha]_D$: -57.1 (*c* 1.00, $CHCl_3$), 97% ee (calculated by chiral GC of ketone (+)-**2** obtained after oxidation with PCC) (reported [16]: MP 90-92ºC; $[\alpha]_D$: -45.3).

(1*S*,3*S*,4*R*)-(+)-3-Hydroxy-1,8-cineole, (+)-**3** and **(1*S*,3*S*,4*R*)-(+)-3-Acetyloxy-1,8-cineole,** (+)-**4:** (150 mg, 0.70 mmol) was refluxed for 2 h with 3% KOH in ethanol (3 mL). After cooling, the reaction mixture was diluted with brine (10 mL), acidified with 5% HCl and thoroughly extracted with $CHCl_3$. After the usual workup and final purification by flash CC on Sil gel, (1*S*,3*S*,4*R*)-(+)-3-hydroxy-1,8-cineole (+)-**3** was isolated (115 mg, 95.6%), as a crystalline solid, MP: 93-94ºC (from pentane); $[\alpha]_D$: +56.2 (*c* 1.00, $CHCl_3$), 94% ee (calculated by chiral GC of the (-)-**2** ketone obtained after oxidation with PCC) (reported [16] MP: 90-92ºC $[\alpha]_D$: +49.8).

(1*R*,4*R*)-(+)-3-Oxo-1,8-cineole, (+)-**2** and **(1*S*,4*S*)-(-)-3-Oxo-1,8-cineole**, (-)-**2:** To a stirred suspension of pyridinium chlorochromate (PCC) (187 mg, 0.87 mmol) in CH_2Cl_2 (2 mL) was added dropwise a solution of (1*R*,3*R*,4*S*)-(-)-3-hydroxy-1,8-cineole (-)-**3** (100 mg, 0.59 mmol) or (1*S*,3*S*,4*R*)-(+)-3-hydroxy-1,8-cineole (+)-**3** (100 mg, 0.59 mmol) in CH_2Cl_2 (1.5 mL) at room temperature. The resulting suspension was stirred for 2 h, diluted with anhydrous ether (6 mL), the supernatant decanted, and the gummy residue extracted with ether (3 x 8 mL). The organic extracts were reunited and filtered through a short pad of Florisil. After solvent evaporation, the residue was chromatographed through a silica gel column (hexane:EtOAc, 49:1) to yield (1*R*,4*R*)-(+)-3-oxo-1,8-cineole (+)-**2** from (-)-**3** (84 mg, 85%) as a colorless oil, $[\alpha]_D$: +36.7 (*c* 5.00, $CHCl_3$), 97% ee; and (1*S*,4*S*)-(-)-3-oxo-1,8-cineole (-)-**2** from (+)-**3** (79 mg, 80%), as a colorles oil, $[\alpha]_D$: -33.6 (*c* 5.00, $CHCl_3$), 94% ee showing NMR and MS data identical to those reported [6].

(±)-3,5-*cis*,*cis*-Diacetyloxy-1,8-cineole 5: The symmetric diketone 3,5-dioxo-1,8-cineole and the *meso*-diol 3,5-*cis*,*cis*-dihydroxy-1,8-cineole were prepared as previously described [6]. *Meso*-diol (506 mg, 2.72 mmol), in anhydrous pyridine (6 mL), was

treated with recently distilled acetic anhydride (2.0 mL, 21 mmol) and allowed to react overnight at room temperature with protection against moisture ($CaCl_2$) and then heated at 70-75ºC (oil bath) for 2 h. The reaction mixture was cooled, treated with 10% HCl (50 mL) and thoroughly extracted with chloroform. The chloroform extracts were washed with a saturated solution of $CuSO_4$, dried (Na_2SO_4), filtered and the solvent evaporated. The residue was flash chromatographed through a short Si gel column with chloroform-ethyl acetate 9:1 to yield 680 mg (93%) of *meso*-diacetate **5** as a crystalline solid, MP: 109-110ºC (from hexane) showing MS, ^{1}H- and ^{13}C-NMR data identical to those reported [27].

(1*S*,3*S*,4*R*,5*R*)-(-)-3-Acetyloxy-5-hydroxy-1,8-cineole, **6**: Diacetate **5** was asymmetrized with PLE following the general procedure described above. From 400 mg (1.48 mmol) of **5** and after incubation for 12 h, 311 mg (92%) of (1*S*,3*S*,4*R*,5*R*)-(-)-3-acetyloxy-5-hydroxy-1,8-cineole **6** were isolated as a colourless oil, $[\alpha]_D$ = -1.56 (*c* 5.71, $CHCl_3$) showing MS, ^{1}H- and ^{13}C-NMR data identical to those reported for the racemic compound [27]. Chiral GC of the asymmetrized hydroxy-acetate **6** using oven temperature program (b) showed a single peak with Rt 33.8 min while a racemic synthetic sample [27] displayed two almost baseline resolved peaks at 33.6 min and 33.8 min. The absolute configuration of the asymmetrized hydroxy-acetate **6** was determined by the Mosher method [20,21] and, as could be anticipated, it resulted to be 1*S*,3*S*,4*R*,5*R*. The NMR data for the (*R*)- and (*S*)-MPTA esters of **6** are given in Table 2.

(1*R*,3*S*,4*R*)-(+)-3-Acetyloxy-5-oxo-1,8-cineole 7: PCC oxidation of **6** (151 mg, 0.66 mmol) following the same procedure as just described to prepare (+)-**2** and (-)-**2** afforded (1*R*,3*S*,4*R*)-(+)-3-acetyloxy-5-oxo-1,8-cineole **7** (136 mg, 91% yield) as prisms.
MP: 100-102ºC.
$[\alpha]_D$: +84.7 (*c* 4.25, $CHCl_3$).
^{1}H- and ^{13}C-NMR: Table 2.
MS (EI, 70 eV, direct inlet): m/z (%) 227 [M^++ H] (38), 211 (43), 167 (8), 151 (11), 149 (4), 125 (28), 109 (100), 108 (9), 83 (26), 82 (15), 81 (13), 79 (11), 67 (13), 55 (6).
Chiral GC analysis using oven temperature program (c) showed a single peak, Rt 17.94 min.

VCD Measurements: VCD spectra were measured using a BioTools BOMEM chiralIR spectrophotometer equipped with a single photoelastic modulator. Samples of each enantiomer were dissolved in 150 µL of CCl_4, placed in a BaF_2 cell with a pathlength of 75 µm and data were acquired at a resolution of 4 cm^{-1} during 3 h. For (+)-**2**, 8.2 mg were used, while for (-)-**2**, 13.6 mg were measured. Baseline corrections were done either by substracting the spectra from the solvent or from a sample of 8.4 mg of (±)-**2** in 150 µL of CCl_4.

Molecular modeling: Geometry optimizations for (-)-**3** and (-)-**6** MTPA esters were carried out using a Monte Carlo protocol [22] at MMFF94 level. A total of 7, 8, 12, and 11 conformers for (-)-**3** (*R*)-MTPA, (-)-**3** (*S*)-MTPA, (-)-**6** (*R*)-MTPA, and (-)-**6** (*S*)-MTPA esters, respectively, were found with a $\Delta E = 2$ kcal/mol in a 10 kcal/mol range. In order to obtain the most stable conformer, all structures were reoptimized by DFT [18] at the B3LYP/6-31G(d) level of theory using the Spartan'04 program routines.

Geometry optimizations for (1*S,*4*S*)-**2** was carried out using the MMFF94 force-field calculations. The E_{MMFF94} value was used as the convergence criterion, and a further search with the Monte Carlo protocol [22] was carried out with no restriction. Only one structure was located and re-optimized using DFT [18] at the B3LYP/6-31G(d) level of theory *via* Spartan'04W software routines. Final geometry optimization and calculation of IR and VCD frequencies for (1*S,*4*S*)-**2** at the DFT B3LYP/DGDZVP level of theory was then performed using Gaussian 03W software. No solvent effects were included in the calculations. The DFT B3LYP/DGDZVP calculation required 14 h of computational time using a desktop personal computer with 2 GB RAM operated at 3 GHz.

Odor characteristics
Alcohols:
(1*R*,3*R*,4*S*)-(-)-**3**: camphoraceous, sweet.
(1*S*,3*S*,4*R*)-(+)-**3**: spicy (weak).
Ketones
(1*R*,4*R*)-(+)-**2**: sweet, cineole-like (weak).
(1*S*,4*S*)-(-)-**2**: spicy.
Acetates
(1*R*,3*R*,4*S*)-(-)-**4**: woody.
(1*S*,3*S*,4*R*)-(+)-**4**: camphor-like, smooth.

Acknowledgements - This work was supported by Consejo Nacional de Investigaciones Científicas y Técnicas de Argentina (CONICET-PIP 5176/04) and Consejo de Investigaciones de la Universidad

Nacional de Tucumán (CIUNT, research grants 26/D416 and 26/D458). Partial financial support from CONACYT and SIP-IPN Mexico, is also acknowledged. The authors are also grateful to Dr. A. C. Muro for optical rotation measurements.

Supporting information available: A table showing the torsional angles obtained for the most stable conformers of **3R**, **3S**, **6R** and **6S** is available on request.

References

[1] (a) Abbott P, Abbott T. (**2005**) *Eucalyptus oil: Australia's Natural Wonder*. Felton Grimwade & Bickford Pty Ltd., Melbourne; (b) Harborne JB, Baxter H (eds) (**1993**) *Phytochemical Dictionary, A Handbook of Bioactive Compounds from Plants*. Taylor and Francis, London; (c) Zrira S, Bessiere JM, Menut C, Elamrani A, Benjilali B. (**2004**) Chemical composition of the essential oil of nine *Eucalyptus* species growing in Morocco. *Flavour and Fragrance Journal*, ***19***, 172-175; (d) Bignell CM, Dunlop PJ, Brophy JJ, Jackson JF (**1996**) Volatile leaf oil of some South-westerrn and Southern Australian Species of the Genus *Eucalyptus*. Part XII. A. Subgenus Eudesmia: B. Subgenus Symphyomyrtus: Section Exsertaria; Series Globulares. *Flavour and Fragrance Journal*, ***11***, 145-151; (e) Gûenther E. (**1949**) *The Essential Oils*. Van Nostrand Reinhold Co. New York, vol. ***II***, 708.

[2] (a) Laude EA, Morice AH, Grattan TJ. (**1994**) The antitussive effects of menthol, camphor and cineole in conscious guinea-pigs. *Pulmonary Pharmacology*, ***7***, 179-184; (b) Tzakou O, Pitarokilli D, Chinou IB, Harvala C. (**2001**) Composition and antimicrobial activity of the essential oil of *Salvia ringens*. *Planta Medica*, ***67,*** 81-83; (c) Coppen JW. (**2002**) Production, trade and markets for eucalyptus oils. In *Eucalyptus: The genus Eucalyptus*, Medicinal and Aromatic Plants-Industrial Profiles, vol. 22, Coppen JW (Ed). Taylor & Francis, London; (d) Miyazawa M, Shindo M, Shimada T. (**2001**) Oxidation of 1,8-cineole, the monoterpene cyclic ether originated from *Eucalyptus polybractea*, by cytochrome P450 3A enzymes in rat and human liver microsomes. *Drug Metabolism and Disposition*, ***29***, 200-205.

[3] Simonsen JL. (**1953**) The Terpenes. Cambridge University Press, Vol ***1***, 423-432.

[4] Silvestre AJD, Cavaleiro JAS. (**1996**) 1,8-Cineole: applications, metabolism and chemical transformations. *Revista Farmacéutica*, ***138***, 49-57.

[5] De Martinez MV, De Venditti FG, De Fenik IJS, Catalán, CAN. (**1982**) Oxidation of 1,8-cineole with chromyl acetate. Some new oxygenated derivatives of 1,8-epoxy-*p*-menthane. *Journal of the Argentine Chemical Society*, ***70***, 137-148.

[6] De Boggiatto MV, De Heluani CS, De Fenik IJS, Catalán CAN. (**1987**) Regiospecific functionalization of the monoterpene ether 1,3,3-trimethyl-2-oxabicyclo[2.2.2]octane (1,8-cineole). Synthesis of the useful bridged γ-lactone 1,3-dimethyl-2-oxabicyclo[2.2.2]octan-3→5-olide. *Journal of Organic Chemistry*, ***52***, 1505-1511.

[7] Villecco MB, Muro AC, Catalán, JV, Catalán CAN. (**2005**) Capítulo IX. Síntesis de derivados de 1,8-cineol, cariofileno y cariolan-1-ol con utilidad en perfumería y farmacología. In *Plantas Iberoamericanas como fuente de terpenoides útiles en química fina*. A. Fernández Barrero (Ed). ISBN 84-96023-32-x Programa CYTED, Granada, Spain, 189-211.

[8] (a) Mac Rae IA, Alberts V, Carman RM, Shaw IM. (**1979**) Products of 1,8-cineole oxidation by a *Pseudomonas. Australian Journal of Chemistry*, ***32***, 917-922; (b) Carman RM, MacRae IC, Perkins MV. (**1986**) The oxidation of 1,8-cineole by *Pseudomonas flava*. *Australian Journal of Chemistry*, ***39***, 1739-1746; (c) Liu WG, Rosazza JPN. (**1990**) Stereospecific hydroxylation of 1,8-cineole using a microbial catalyst. *Tetrahedron Letters*, ***31***, 2833-2836; (d) Trudgill PW. (**1990**) Microbial metabolism of monoterpenes-recent developments. *Biodegradation*, ***1***, 93-105; (e) Rasmussen JAM, Henderson KA, Straffon MJ, Dumsday GJ, Coulton J, Zachariou M. (**2005**) Two new biocatalysts for improved biological oxidation of 1,8-cineole. *Australian Journal of Chemistry*, ***58***, 912-916.

[9] (a) Southwell IA. (**1975**) Essential oil metabolism in the koala. III Novel urinary monoterpenoid lactones. *Tetrahedron Letters*, ***24***, 1885-1888; (b) Boyle R, McLean S, Foley W, Davies NW, Peacock EJ, Moore B. (**2001**) Metabolites of dietary 1,8-cineole in the male koala (*Phascolarctos cinereus*). *Comparative Biochemistry and Physiology Part C*, ***129***, 385-395; (c) Boyle R, McLean S, Davies NW. (**2000**) Biotransformation of 1,8-cineole in the brushtail opossum (*Trichosurus vulpecula*). *Xenobiotica*, ***30*,** 915-932; (d) Flynn TM, Southwell IA. (**1979**) 1,3-Dimethyl-2-oxabicyclo[2.2.2]octane-3-methanol and 1,3-Dimethyl-2-oxabicyclo[2.2.2]octane-3-carboxylic acid, urinary metabolites of 1,8-cineole. *Australian Journal of Chemistry*, ***32***, 2093-2095; (e) Miyazawa M, Kameoka H, Morinaga K, Negoro K, Mura N. (**1989**) Hydroxycineole: four new metabolites of 1,8-cineole in rabbits. *Journal of Agricultural and Food Chemistry*, ***37***, 222-226.

[10] Bitteur, SM, Baumes RL, Bayonove CL, Versini G, Martin CA, Dalla Serra A. (**1990**) 2-exo-Hydroxy-1,8-cineole: A new component from grape var. Sauvignon*. Journal of Agricultural and Food Chemistry*, ***38***, 1210-1213.

[11] Southwell IA, Russel MF, Maddox CDA, Wheeler GS. (**2003**) Differential metabolism of 1,8-cineole in insects. *Journal of Chemical Ecology*, ***29***, 83-94.

[12] Duisken M, Sandner F, Blömeke B, Hollender J. (**2005**) Metabolism of 1,8-cineole by human cytochrome P450 enzymes: Identification of a new hydroxylated metabolite. *Biochimica et Biophysica Acta*, ***1722***, 304-311.

[13] Rodriguez P, Sierra W, Rodriguez S, Menendez P. (**2006**) Biotransformation of 1,8-cineole, the main product of *Eucalyptus* oils. *Electronic Journal of Biotechnology*, ***9***, 232-236.

[14] Williams RD, Trudgill PW, Taylor DG. (**1989**) Metabolism of 1,8-cineole by *Rhodococcus* species: Ring cleavage reactions. *Journal of General Microbiology*, ***135***, 1957-1967.

[15] (a) Kubota K, Nakamura K, Kobayashi A. (**1998**) Acetyloxy-1,8-cineoles as aroma constituents of *Alpinia galanga* Willd. *Journal of Agricultural and Food Chemistry*, ***46***, 5244-5247; (b) Kubota K, Someya Y, Yoshida R, Kobayashi A, Morita T, Koshino H. (**1999**) Enanatiomeric purity and odor characteristics of 2- and 3-acetyloxy-1,8-cineoles in the rhizomes of *Alpinia galanga* Willd. *Journal of Agricultural and Food Chemistry*, ***47*****,** 685-689; (c) Miyasawa M, Hashimoto Y. (**2002**) Antimicrobial and bactericidal activities of esters of 2-*endo*-hydroxy-1,8-cineole as new aroma chemicals. *Journal of Agricultural and Food Chemistry*, ***50***, 3522-3526.

[16] Luzzio FA, Duveau DY. (**2002**) Enzymatic resolution of the 1,3,3-trimethyl-2-oxabicyclo[2.2.2]octane (1,8-cineole) system. *Tetrahedron Asymmetry*, ***13***, 1173-1180.

[17] Loandos MH, Muro AC, Villecco MB, Catalán CA. (**2006**) Stereospecificity of pig liver esterase in the hydrolysis of racemic esters derived from 1,8-cineole. *Molecular Medicinal Chemistry*, ***10***, 35-37.

[18] (a) Perdew JP. (**1986**) Density-functional approximation for the correlation energy of the inhomogeneous electron gas. *Physical Reviews* B, ***33***, 8822-8824; (b) Godbout N, Salahud DR, Andzelm J, Wimmer E. (**1992**) Optimization of Gaussian-type-basis sets for local spin functional calculations. Part 1. Boron through neon, optimization technique and validation. *Canadian Journal of Chemistry*, ***70***, 560-571; (c) Andzelm J, Wimmer EJ. (**1992**) Density functional Gaussian-type-orbital approach to molecular geometries, vibrations, and reaction energies. *Journal of Chemical Physics*, ***96***, 1280-1303.

[19] Because the peaks of the enantiomeric acetates (+)-**4** and (-)-**4** are not baseline resolved, chiral GC quantization below 1.5% could not be done as the peak of the minor enantiomer is swallowed by the much larger peak of the major enantiomer. On the other hand, a very accurate enantiomer quantization could be made on enantiomeric ketones (+)- and (-)-**2** as they were nicely resolved giving acute and baseline-separated peaks.

[20] Dale JA, Mosher HS. (1973) Nuclear magnetic resonance enantiomer reagents. Configurational correlations *via* nuclear magnetic resonance chemical shifts of diastereoisomeric mandelate, O-methylmandelate, and α-methoxy-α-trifluoromethylphenylacetate (MTPA) esters. *Journal of the American Chemical Society*, ***95***, 512-519.

[21] Preite MD. (**1994**) Determinación de excesos enantioméricos y asignación de configuraciones absolutas por análisis de resonancia magnética nuclear. *Química Nova*, ***17***, 137-151.

[22] Chang G, Guida WC, Still WC. (**1989**) An internal-coordinate Monte Carlo method for searching conformational space. *Journal of the American Chemical Society*, ***111***, 4379-4386.

[23] (a) Halgren T. (**1996**) Merck molecular force field. I. Basis, form, scope, parameterization, and performance of MMFF94, *Journal of Computational Chemistry*, ***17***, 616-641; (b) Halgren TA. (**1996**) Merck molecular force field. II. MMFF94 van der Waals and electrostatic parameters for intermolecular interactions. *Journal of Computational Chemistry*, ***17***, 587-615; (c) Halgren TA. (**1996**) Merck molecular force field. III. Molecular geometries and vibrational frequencies for MMFF94. *Journal of Computational Chemistry*, ***17***, 553-586; (d) Halgren TA. (**1996**) Merck molecular force field. V. Extension of MMFF94 using experimental data, additional computational data, and empirical rules. *Journal of Computational Chemistry*, ***17***, 490-519.

[24] (a) Godbout N, Salahud DR, Andzelm J, Wimmer E. (**1992**) Optimization of Gaussian-type-basis sets for local spin functional calculations. Part 1. Boron through neon, optimization technique and validation. *Canadian Journal of Chemistry*, ***70***, 560-571. (b) Andzelm J, Wimmer EJ. (**1992**) Density functional Gaussian-type-orbital approach to molecular geometries, vibrations, and reaction energies. *Journal of Chemical Physics*, ***96***, 1280-1303.

[25] (a) Rojas-Pérez R, Cedillo-Portugal E, Joseph-Nathan P, Burgueño-Tapia E. (**2009**) A new longipine diester from *Stevia monardifolia* Kunth. *Natural Product Communications*, ***4***, 757-762; (b) Muñoz MA, Areche C, San-Martín A, Rovirosa J, Joseph-Nathan P. (**2009**) VCD determination of the absolute configuration of stypotriol. *Natural Product Communications*, ***4***, 1037-1040.

[26] Villecco MB, Hernández LR, Guzmán MI, Catalán CAN, Bucio MA, Joseph-Nathan P. (**2001**) Synthesis, stereochemistry and absolute configuration of deodarols and deodarones. *Tetrahedron Asymmetry*, ***12***, 2947-2953.

[27] Villecco MB, Catalán JV, Vega MI, Garibotto FM, Enriz RD, Catalán CAN. (**2008**) Synthesis and antibacterial activity of highly oxygenated 1,8-cineole derivatives. *Natural Product Communications*, ***3***, 303-312.

Original Paper

Letter to Editor

Natural Product Communications
2009
Volume 4, Number 11

Contents

Chemical Biodiversity of Secondary Metabolites from Endophytic Fungi

Continued inside backcover